

Charmonium and Heavy Flavour Production at LHCb

Conor Fitzpatrick*

University of Edinburgh, Edinburgh, U.K.

E-mail: conor.fitzpatrick@cern.ch

On behalf of the LHCb collaboration

The underlying mechanism of prompt charmonium production at hadron colliders is a topic of great interest. Measurements of charmonium production at the Large Hadron Collider beauty (LHCb) experiment for both prompt and secondary $J/\psi(1S)$ events will be compared with theoretical expectation. Results will also be shown for other charmonium states, and for the upsilon system. The LHCb physics programme relies on the reconstruction of the decays of B and D hadrons. An important first step in this program is to demonstrate that this reconstruction can be done with high efficiency, and to establish the production cross-section for these hadrons in pp collisions at $\sqrt{s} = 7$ TeV, which is presented here.

*The Xth Nicola Cabibbo International Conference on Heavy Quarks and Leptons,
October 11-15, 2010
Frascati (Rome) Italy*

*Speaker.

1. Introduction

The LHCb experiment is a precision beauty and charm physics experiment at the Large Hadron Collider (LHC) [1]. It has been designed to search for indirect evidence of new physics in CP violation in rare decays. The LHCb detector adopts a forward-arm spectrometer configuration fully instrumented on $15 < \Theta < 300$ mrad to take advantage of the correlated forward production of b, \bar{b} quark pairs at the LHC. The precise vertexing, efficient particle ID and trigger capabilities of LHCb permit measurements of production cross-sections in a unique region of phase space. Over the course of the 2010 LHC running period LHCb recorded $\sim 37 \text{ pb}^{-1}$ of pp collisions. This note describes measurements made with up to 0.6 pb^{-1} of this data.

2. Quarkonia

Muons are present in the final states of many CP-sensitive B decays and are of particular interest in a number of semileptonic modes where they provide a tag of the initial state flavor of accompanying neutral B mesons. As such the muon system of LHCb provides a crucial role in the triggering and offline identification of muons as used in the quarkonia analyses.

2.1 Inclusive $J/\psi(1S)$ production

$J/\psi(1S)$ cross-section measurements are of particular interest as they present a new opportunity to test the inclusion of color octet effects in NRQCD predictions. $J/\psi(1S)$ mesons are produced at the LHC through direct pp production, feed-down from heavier charmonia such as χ_c and $\psi(2S)$ mesons and from longer lived particles such as b hadrons. LHCb presents the inclusive $J/\psi(1S) \rightarrow \mu^- \mu^+$ cross-section on the momentum and rapidity range $p_T < 10 \text{ GeV}/c$, $2.5 < y < 4$ with 14 nb^{-1} [2]. The efficiency of selecting a $J/\psi(1S)$ meson is dependent upon its polarisation, which ignoring the azimuthal dependence is of the form:

$$\frac{dN}{d\cos\theta} = \frac{1 + \alpha \cos^2\theta}{2 + 2 \times \alpha/3}$$

where θ is the angle between the positive muon momentum direction in the $J/\psi(1S)$ CM frame and the $J/\psi(1S)$ momentum direction in the Lab frame. The inclusive cross-section is determined to be

$$\sigma(\text{pp} \rightarrow J/\psi(1S)X) = (7.65 \pm 0.19 \pm 1.10_{-1.27}^{+0.87}) \mu\text{b}$$

where the first uncertainty is statistical, the second systematic and we assume $\alpha = 0$ with the undetermined polarisation appearing as a two-sided systematic uncertainty using the extreme $\alpha = 1, -1$ cases. Comparison to the LHCb PYTHIA tune using both PYTHIA 6.3 colour singlet and PYTHIA 6.4 with colour octet [3] is shown in figure 1. Both simulations show poor agreement with the measurement. We are updating the result for publication with $\sim 6 \text{ pb}^{-1}$ and future studies include a polarisation measurement with the full dataset.

2.2 χ_c and $\psi(2S)$ measurements

With the data collected this year, LHCb will measure production cross-sections for χ_c and $\psi(2S)$ mesons. The process $\chi_c \rightarrow J/\psi(1S)\gamma$ is of interest as we expect that $\sim 40\%$ of $J/\psi(1S)$

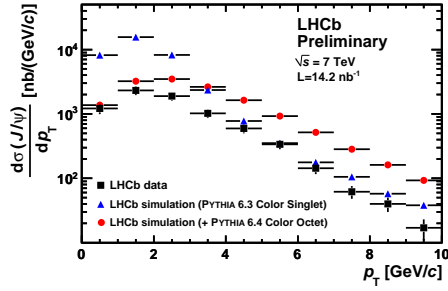


Figure 1: $J/\psi(1S)$ inclusive cross-section in bins of transverse momentum, p_T , compared to the LHCb MC simulation using PYTHIA 6.3 and PYTHIA 6.4 including colour octet.

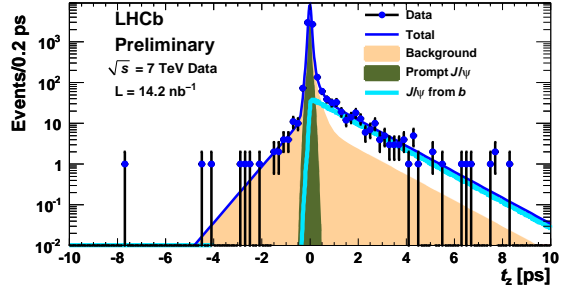


Figure 2: The pseudo-proper time distribution of $J/\psi(1S)$ candidates selected as part of the $J/\psi(1S)$ inclusive cross-section measurement.

at LHCb come from χ_c . Of additional interest are the cross-section ratios $\sigma(\chi_c)/\sigma(J/\psi(1S))$, $\sigma(\chi_{c1}(1P))/\sigma(\chi_c)$, $\sigma(\chi_{c2}(1P))/\sigma(\chi_c)$ which will be measured both for prompt χ_c and χ_c from b hadrons. $\psi(2S)$ has essentially no feed-down from higher quarkonia states which leads to more straightforward interpretation than that of $J/\psi(1S)$ and as such is a subject of great interest. LHCb has observed both $\psi(2S) \rightarrow \mu^- \mu^+$ and $\psi(2S) \rightarrow J/\psi(1S) \pi^+ \pi^-$ as shown in figure 3.

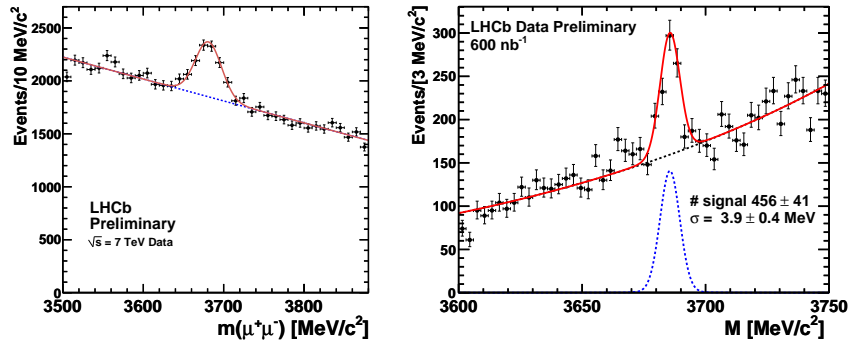


Figure 3: The invariant mass distributions of $\psi(2S) \rightarrow \mu^- \mu^+$ (left) and $\psi(2S) \rightarrow J/\psi(1S) \pi^+ \pi^-$ (right) with the first 600 nb^{-1} of data recorded at $\sqrt{s} = 7$ TeV by the LHCb experiment.

2.3 Heavier charmonia

The $X(3872)$ and $Z(4430)^\pm$ states are of great interest and have been the subject of simulation based sensitivity studies at LHCb [4, 5], with future plans including angular analysis of $B^+ \rightarrow X(3872)K^+$ where $X(3872) \rightarrow J/\psi(1S)\rho^0$. For the mode $X(3872) \rightarrow J/\psi(1S)\pi^+\pi^-$ the $\psi(2S)$ analysis provides a cross-check. An angular analysis of $X(3872)$ from B^+ will permit extraction of the quantum numbers of this state, which are as yet unmeasured. An additional advantage of using $X(3872)$ from B^+ is that it permits separation from the primary vertex resulting in reduced combinatoric backgrounds. LHCb is studying the $X(3872)$ and results will be presented soon.

2.4 The Υ system

LHCb has observed the Υ 1S, 2S and 3S resonances decaying to muon pairs with the first 600 nb⁻¹. We obtain a mass resolution of ~ 50 MeV/c² as shown in Figure 4, permitting separate measurement of the 1S, 2S and 3S states. With the full dataset recorded this year we expect to publish a cross-section measurement in bins of p_T for the $\Upsilon(1S)$, and since the presentation of this talk further alignment and calibration has reduced the mass resolution to ~ 47 MeV/c².

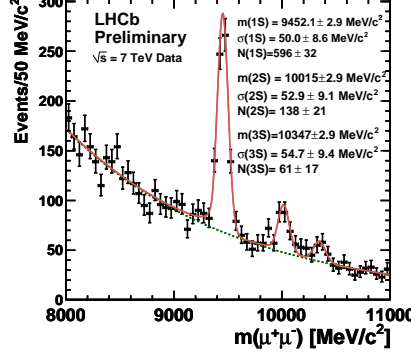


Figure 4: The invariant dimuon mass spectrum showing the Υ system as measured with the first 600 nb⁻¹ of data recorded at $\sqrt{s} = 7$ TeV by the LHCb experiment. The 1S, 2S and 3S states are all visible and well separated, with a resolution of ~ 50 MeV.

3. $b\bar{b}$ Production

3.1 $\sigma(pp \rightarrow b\bar{b}X)$ cross-section using inclusive $J/\psi(1S)$ decays

The inclusive $J/\psi(1S)$ cross-section measurement permits discrimination between $J/\psi(1S)$ from b-hadrons and short-lived states through the pseudo-proper-time variable (t_z):

$$t_z = \Delta z \times \frac{M_{J/\psi}}{p_z}$$

where p_z is the $J/\psi(1S)$ momentum component and Δz the distance between primary and secondary vertices along the beam axis respectively. We show the t_z distribution in Figure 2 in which the prompt signal component is described as a delta function at $t_z = 0$ and the signal component from b-hadrons as an exponential decay. These are convolved with a double Gaussian resolution function. The background distribution is determined from the sidebands of the $J/\psi(1S)$ mass distribution. An extended maximum likelihood fit results in the fraction of $J/\psi(1S)$ from b, denoted $f_b = 11.1 \pm 0.8\%$. Using this fraction and the inclusive $J/\psi(1S)$ cross-section the cross-section for $J/\psi(1S)$ from b-hadrons on the transverse momentum and rapidity range $p_T < 10$ GeV/c, $2.5 < y < 4$ is determined to be $0.81 \pm 0.06 \pm 0.13$ μb [2]. This is extended using PYTHIA to the average cross-section to produce b or \bar{b} flavoured hadrons, H_b , within the LHCb acceptance:

$$\sigma(pp \rightarrow H_b X) = (84.5 \pm 6.3 \pm 15.6) \mu\text{b} \quad (2 < \eta < 6)$$

Where η is the pseudorapidity of the b-hadron. A further extrapolation is made to the $b\bar{b}$ production cross-section yielding:

$$\sigma(pp \rightarrow b\bar{b}X) = (319 \pm 24 \pm 59) \mu\text{b}$$

In both cases the first error is statistical and the second systematic. No additional uncertainty is assigned to the extrapolation method.

3.2 $\sigma(pp \rightarrow b\bar{b}X)$ cross-section using $D^0 X \mu^- \bar{\nu}_\mu$ decays.

The $b\bar{b}$ production cross-section using decays of b-hadrons to final states containing a D^0 meson and a muon are the subject of the first LHCb publication at $\sqrt{s} = 7$ TeV [6]. For this analysis two trigger configurations are used, forming two separate datasets. The size of these datasets are 2.9 nb^{-1} and 12.2 nb^{-1} , and the final result is averaged over both measurements which are consistent within errors. $D^0 X \mu^- \bar{\nu}_\mu$ candidates are selected by requiring a kaon and a pion as determined by the particle ID of the LHCb Ring Imaging Cherenkov (RICH) detectors to both have transverse momentum greater than $300 \text{ MeV}/c$ and point towards a common vertex. These $D^0 \rightarrow K^- \pi^+$ candidates are required to be detached from the primary vertex with a flight distance significance cut. The D^0 candidates are then matched to a muon track. In order to discriminate between D^0 candidates from $pp \rightarrow c\bar{c}X$ and those produced from $pp \rightarrow b\bar{b}X$ the Impact Parameter (IP) with respect to the primary vertex is used. Candidates produced from the decay of b hadrons, denoted "D⁰ from b" (Dfb) have a larger IP than those from charm, denoted "prompt". A simultaneous log-likelihood fit to the natural logarithm of the IP distribution and D^0 mass distribution is sufficient to determine the yield of $D^0 \mu^-$ from b-hadrons: The prompt component shape is determined from an enriched selection of prompt D^0 candidates which are required to point to the primary vertex. The Dfb component shape is determined from MC. As an additional cross-check "Wrong Sign" (WS) candidates are reconstructed in which the kaon from D^0 and muon have opposite charges. As this mode is highly suppressed in semileptonic b decays it may be used to further constrain the shape of the background component of the IP distribution. The fit to the $\ln(\text{IP})$ distributions for right-sign and wrong-sign candidates is shown in Figure 5. The simultaneous fit is performed in bins of

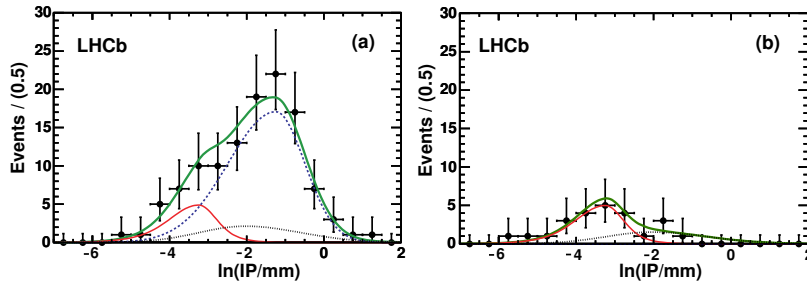


Figure 5: The natural logarithm of the impact parameter distribution for D^0 candidates with respect to the primary vertex for (a) right-sign $D^0 \mu^-$ candidates and (b) wrong-sign $D^0 \mu^+$ candidates as selected from the 2.9 nb^{-1} microbias-triggered sample. In blue is the Dfb component of the fit, in red prompt D^0 candidates and in grey background as determined from sidebands.

pseudorapidity on the range $2 < \eta < 6$ for both datasets. Selection and trigger efficiencies are determined from MC and corrected for MC-data differences by studying $J/\psi(1S) \rightarrow \mu^- \mu^+$ decays for

the muon-triggered sample. The efficiency-corrected yields are then translated into cross-sections and compared to two theories, MCFM [7] and FONLL[8]. The cross-section in bins of η are presented in Figure 6. Summing over η the average cross-sections in η we measure:

$$\sigma(pp \rightarrow H_b X) = (75.3 \pm 5.4 \pm 13.0) \mu\text{b} \quad (2 < \eta < 6)$$

where the first uncertainty is statistical and the second systematic. Extrapolating to the full η range using PYTHIA to determine the acceptance correction results in a total $b\bar{b}$ cross-section of

$$\sigma(pp \rightarrow b\bar{b} X) = (284 \pm 20 \pm 49) \mu\text{b}$$

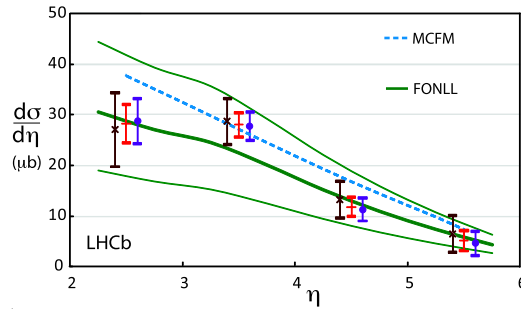


Figure 6: $\sigma(pp \rightarrow H_b X)$ as a function of η for (brown crosses) microbias-triggered (blue circles) muon-triggered and (red pluses) average of both datasets compared to MCFM (blue, dashed) and FONLL (green, solid) theory calculations for the $D^0 X \mu^- \bar{\nu}_\mu$ analysis.

3.3 $\sigma(pp \rightarrow b\bar{b} X)$ cross-section using $D^{*-} \mu^+ \nu_\mu X$ decays.

A separate analysis to the $D^0 X \mu^- \bar{\nu}_\mu$ has also been performed using $D^{*-} \mu^+ \nu_\mu X$ with 14.9 nb^{-1} . The selection is optimised for the channel $B^0 \rightarrow D^{*-} \mu^+ \nu_\mu X$ with $D^{*-} \rightarrow \bar{D}^0 \pi^-$ where $\bar{D}^0 \rightarrow K^+ \pi^-$. Final states with additional particles that are not explicitly reconstructed are also included. The yield of $D^{*-} \mu^+$ is determined from a 2-dimensional simultaneous fit to both the \bar{D}^0 mass and the $D^{*-} - \bar{D}^0$ mass difference, permitting removal of \bar{D}^0 candidates that did not come from D^{*-} . In a strategy similar to that of the $D^0 X \mu^- \bar{\nu}_\mu$ analysis, the yield of D^{*-} candidates coming from b is determined in a fit to the log(IP) distribution. The cross-section for B^0 mesons is determined and extended to the inclusive b-hadron cross-section:

$$\sigma(pp \rightarrow b\bar{b} X) = (73 \pm 12 \pm 17) \mu\text{b} \quad (2 < \eta < 6)$$

and extending to the full-phase space:

$$\sigma(pp \rightarrow b\bar{b} X) = (275 \pm 44 \pm 66) \mu\text{b}$$

4. Open Charm

In addition to charmonia, LHCb has measured production cross-sections of a number of open-charm mesons in bins of p_T and rapidity: $D^{*+} \rightarrow \pi^+ D^0 (K^- \pi^+)$, $D^0 \rightarrow K^- \pi^+$, $D^+ \rightarrow K^- \pi^+ \pi^+$,

$D_s^+ \rightarrow \phi(K^+K^-)\pi^+$ using 1.8 nb^{-1} with an extension to 14 nb^{-1} ongoing [9]. In this analysis the log(IP) distribution is once again used, this time with the intention of specifically selecting prompt open charm. The cross-section ratio $\sigma(D^+)/\sigma(D_s^+)$ has been measured in bins of p_T as shown in Figure 4: This is found to be flat, and a fit to this distribution furnishes the result:

$$\sigma(D^+)/\sigma(D_s^+) = 2.32 \pm 0.27 \pm 0.26$$

This is consistent with the ratio $f(c \rightarrow D^+)/f(c \rightarrow D_s^+) = 3.08 \pm 0.70$ [10]. The cross-section results are in good agreement with theory predictions from two groups [8, 11] as well as with the LHCb PYTHIA tune.

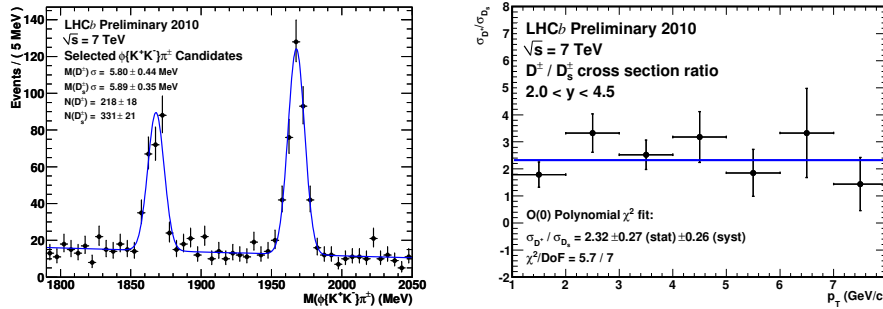


Figure 7: $M(\phi\pi^+)$ fit (left) from which the (right) $\sigma(D^+)/\sigma(D_s^+)$ cross-section ratio is determined with the first 1.8 nb^{-1} of data recorded at $\sqrt{s} = 7 \text{ TeV}$ by the LHCb experiment.

References

- [1] LHCb Collaboration, *The LHCb Detector at the LHC*, *JINST* **3** (2008) S08005.
- [2] LHCb Collaboration, *Measurement of the J/ψ production cross section at $\sqrt{s} = 7 \text{ TeV}$ in LHCb*, Oct, 2010. LHCb-CONF-2010-010. CERN-LHCb-CONF-2010-010.
- [3] M. Bargiotti and V. Vagnoni, *Heavy Quarkonia sector in PYTHIA 6.324: tuning, validation and perspectives at LHC(b)*, Jun, 2007. LHCb-2007-042. CERN-LHCb-2007-042.
- [4] N. Mangiafave, J. Dickens, and V. Gibson, *A Study of the Angular Properties of the $X(3872) \rightarrow J/\psi\pi^+\pi^-$ Decay*, Jan, 2010. LHCb-PUB-2010-003. CERN-LHCb-PUB-2010-003.
- [5] L. Nicolas and O. Schneider, *Alignment of the LHCb Tracking Stations and Selection of $X(3872)$ and $Z(4430)^\pm$ in pp Collisions at 14TeV* . PhD thesis, Lausanne, EPFL, 2009. Presented on 26 Nov 2009.
- [6] LHCb Collaboration, *Measurement of $\sigma(pp \rightarrow b\bar{b}X)$ at $\sqrt{s} = 7 \text{ TeV}$ in the forward region*, *Phys. Lett.* **B694** (2010) 209–216, [[arXiv:1009.2731](https://arxiv.org/abs/1009.2731)].
- [7] J. Campbell and K. Ellis, “MCFM: Monte Carlo for FeMtobarn processes.” See <http://mcfm.fnal.gov/> for details.
- [8] M. Cacciari, S. Frixione, M. Mangano, P. Nason, and G. Ridolfi, *private communication*, 2010.
- [9] LHCb Collaboration, *Prompt charm production in pp collisions at $\sqrt{s} = 7 \text{ TeV}$* , Oct, 2010. LHCb-CONF-2010-013. CERN-LHCb-CONF-2010-013.
- [10] Particle Data Group Collaboration, C. Amsler *et al.*, *Review of Particle Physics*, *Phys. Lett.* **B667** (2008) 1. and 2009 partial update for the 2010 edition.
- [11] B. A. Kniehl, G. Kramer, I. Schienbein, and H. Spiesberger, *private communication*, 2010.